# Dust release from aggregative cohesive powders subjected to vibration

*Hamid Salehi*[+]*, Nicoletta Lotrecchiano, Diego Barletta, Massimo Poletto**

Dipartimento di Ingegneria Industriale, Università degli Studi di Salerno

Via Ponte Don Melillo, I-84084 Fisciano (SA), ITALY

[+] Currently at Department of Biomaterial and Technology at Swedish University of Agricultural Science, Umeå, Sweden

*corresponding author: mpoletto@unisa.it

Tel.: +39-089-96-4132; fax: +39-089-96-8781

Keyword: Dust formation, Environmental & workplace protections, Vibrated fluidized bed, Aggregate formation

**ABSTRACT**

Dust release from a mechanical vibrated bed of cohesive powders aerated close to the minimum for fluidization. The material tested were silica and potato starch. The effect of both vibration intensity and of vibration frequency on dust formation are verified and a model to account for these two variables has been developed. A dimensionless dust release parameter has been

defined and calculated from the experimental results. This parameter is able to explain the role of the acceleration due to vibration and of cohesive interparticle forces, also accounting for the magnification effects of acceleration intensity close to resonance conditions. However the same parameter is unable to fully account for changes on dust emission induced by fluidized bed bubbling promoted by vibration frequencies close to resonance. Without considering these effects frequency determines a reduction of dust release that should be explained introducing some other effects than those considered in our model.

## 1. INTRODUCTION

Air pollution has become a serious environmental, political and social issue during the last decade, and it creates multiple challenges for both industries and governments. Long term exposure to air pollution could lead to serious health problems. Particular Matters (PMn) can be carried deep into the lungs and cause lung and heart diseases. The Parliament Hill Research Ltd [1] reported 620 death in central London due to PMn exposure.

A large majority of raw materials, intermediate and final products used in different industrial applications, i.e. food, pharmacy, metallurgy, chemistry and mineral industries are solids particulates and powders. This is due to several advantages that powders have compared to liquids, *e.g.* transport facility, storage and volume reduction to name but a few. However, concerns over the ecosystem, community and vocational health due to both dust emission and also dust explosion [2] explains the need for new dust formation characterization procedures [3–6]. A large quantity of dust emission in industries usually happen during the conventional handling operations like extraction of a part from its bag, bag agitation, displacement and more importantly transportation of powders [7,8]. In order to control and prevent dust emission three steps should be implemented. Firstly, the tendency of powders to release dust should be

interpreted [9], secondly an appropriate measuring system based on the source of dust generation should be developed [10] and finally dust release modeling has to be performed to measure the quantity of the released dust [11].

Transportation effects on dust emission can be simulated by using vibration. For instance, Saleh *et al*. [12] combine agitation and fluidization in order to assess powder dustiness. Le Bihan *et al.* [13] and Morgeneyer *et al.* [3] used vortex shaker method, which is the mechanical stirring of powder, for the characterization of aerosol. Shandilya *et al*. [14,15] developed a model in order to simulate the aerosol particle emission under the effect of mechanical abrasion. They showed that particle aerosols emission of tested powders is strongly affected by different product formulation.

The use of vibration together with fluidization has been largely studied, with regard to the application of mechanical oscillations [16], of sound waves [17–20] or combination of both [21]. In studies conducted by Chirone *et al.* [22] and Russo *et al.* [23] sound effect on aggregate of cohesive powders at frequencies higher than 100 Hz were studied. Sound was also used to promote the filtration effectiveness of vibrated beds [24,25], and to promote mixing in fluidized beds [26,27]. Furthermore, mechanical vibration shows the capability to break aggregates and other formed structures in fluidized bed which hinder the proper fluidization of group C cohesive powders [28–34]. The generally recognized mechanism, involves the breakage of clumps and aggregates into fragments small enough to be fluidized. Generally this process is able to turns the fluidization behaviour of a Group C powder in to that of a Group A powder, characterized by the presence of a fluidization velocity range of homogeneous fluidization [35–37]. Mechanical vibration were also used to change the elutriation of fines from fluidized beds [38].

In order to understand the process of dust release, it is necessary to elucidate its fundamental physics. With cohesive powders agglomerate formation should be properly accounted for to describe the fundamental physics. In particular, this paper aims at describing and explaining the role of mechanical vibration of fluidized powders in in the release of dust. Two different cohesive powders were fluidized below their minimum fluidization velocity at different frequencies and accelerations ratio. The approaches developed by Barletta *et al*. [39], to analyze aggregates formation in silo discharge, and by Barletta and Poletto [37], to describe the aggregative behavior of cohesive powders in mechanically vibrated fluidized beds, will be used to estimate the aggregate size in the different operating conditions tested. In this paper, however, the proper acceleration imparted to the bed will account for the effective response of the bed depending on the vibration frequency. In turn the aggregate size will be used apply the model developed by Salehi *et al*. [40] to discuss the results.

## 2. THEORETICAL BACKGROUND

It was assumed by Salehi *et al*., [40] that the fine cohesive powders are prone to release dust when they tend to produce aggregates in the powder bed. Aggregation is affecting dust release due to two parameters. In fact, on the one hand aggregates exhibit a surface prone to dust detachment and on the other hand cohesion of particles on the aggregate surface affects dust emission.

Barletta *et al*. [39] assumed that aggregates tend to detach along the horizontal bed surface during the incipient bed expansion in the fluidized state. In particular, aggregate formation occurs when its weight is larger than the attraction force, $F_c$, linking the aggregate to the rest of the powder bed through a number of intra aggregate contact points. The force balance on the aggregate yields:

$$\frac{\pi d_a^3}{6}\rho_a g = F_c \quad (1)$$

where $g$ is the acceleration due to gravity and $d_a$ and $\rho_a$ are the aggregate diameter and density, respectively. It ought to be considered that fluid dynamic forces as well should be accounted for the force balance of Eq. (1). However, it is reasonable to neglect these additional forces since aggregate formation mainly occurs at low gas velocity when the powder is in a fixed bed regime. The attraction force between aggregates $F_c$ can be estimated from powder flow properties, i.e from the tensile strength. In fact, by considering the contact plane between neighbor layers, the tensile strength, $\sigma_t$, and the attraction force $F_c$ are linked as follows:

$$\sigma_t = F_c n_c \quad (2)$$

where $n_c$ is the number of aggregates contacts per unit area in adjacent layers. A possible estimate of $n_c$ is the following:

$$n_c = k d_a^{-2} \quad (3)$$

where $k$ is the number of contacts that an aggregate has with the others contained in an adjacent layer. Literature reports empirical functions for $k$ (ε) in case of rigid spherical particles [41,42]. The maximum value for $k$ at the minimum possible voidage was approximately 3 for spheres. A similar value of $k$ can be assumed suitable even for irregularly shaped aggregates, despite they may show a significantly lower external voidage. Combination of Eqs (1) to (3) lead to an estimating correlation for the aggregate size provided that a suitable value of the bulk tensile strength of the powder is known:

$$\frac{\pi d_a^3}{6}\rho_a g = \frac{\sigma_t d_a^2}{k} \quad (4)$$

For an ideal Coulomb powder, the yield locus is given by the following relation:

$$\tau = \sigma \tan\phi_i + C \quad (5)$$

where $\sigma$ and $\tau$ are the normal and shear stresses on the yield surface, respectively, $\phi_i$ is the angle of internal friction and $C$ is the cohesion. Consistently with the Mohr-Coulomb analysis, the tensile strength, $\sigma_t$, can be estimated by a linear extrapolation of the yield locus in the traction half plane:

$$\sigma_t = -\frac{2C\cos\phi_i}{1+\sin\phi_i} \tag{6}$$

Consolidation affects both the cohesion and the angle of internal friction. As a result, assuming that a very low consolidation applies for an aerated bed, the relevant values of cohesion, $C_0$, angle of internal friction, $\phi_{i0}$, can be estimated by extrapolating values measured by shear testing to negligible consolidation[39,43]. Then, substituting $C_0$ and $\phi_{i0}$, in Eq. (6) the corresponding tensile strength relevant to the fluidized state, $\sigma_{t0}$, can be derived. Moreover, for a gas fluidized bed with mechanical vibrations, it ought to substitute the acceleration due to gravity appearing in Eq (4) with the acceleration due to vibrations, $a$, to obtain the relevant aggregate size:

$$d_a = \frac{6}{k\pi}\frac{\sigma_{t0}}{a\rho_a} \tag{7}$$

The aggregate density can be estimated to be about 1.15 times the vibrated density of the powder according to Zhou and Li [44]. For the sake of simplicity, $\rho_a$ is estimated as follows in this work:

$$\rho_a = m_b / H_0 \Sigma_c \tag{8}$$

where $H_0$ is the bed height under vibrations and without aeration, $U = 0$, $m_b$ is the bed mass and $\Sigma_c$ is the column cross-section.

Salehi *et al.* [40] demonstrated that both particle and bulk properties should be considered in order to properly account for the effect of different scales and of vibration conditions on dust release. In particular, the dust release mass rate, $w_d$, can be related to the number of dust particles

released per unit time, $N_p$, by means of the volumetric average of the particle diameter, $d_{pw}$, and the particle density, $\rho_p$.. As a result, assuming a spherical particle shape, it is:

$$w_d = N_p \rho_p \pi d_{pw}^3 / 6 \tag{9}$$

Firstly, we approach the dust release mechanism at the particle level. The number of released dust particles can be assumed as proportional to area of the external aggregate surface, $A_t$, and to the number density of particles. Therefore, reasonably we have:

$$N_p \propto A_t / d_{pw}^2 \tag{10}$$

The available aggregate area can be calculated from the bed volume:

$$A_t = \left\{ \left[ H_b \frac{\pi D_c^2}{4} (1-\varepsilon_e) \right] \Big/ \frac{\pi d_a^3}{6} \right\} \pi d_a^2 = H_b \frac{\pi D_c^2}{4} (1-\varepsilon_e) \frac{6}{d_a} \tag{11}$$

where $\varepsilon_e$ is the bed voidage external to aggregates and $D_c$ and $H_b$ are the column internal diameter and the bed height, respectively. Following Barletta *et al*.[39], the voidage external to the aggregates $\varepsilon_e$ can be derived from the bulk density, $\rho_b$, and the aggregate density and, thus, from the current bed height, $H$, and the bed height under vibrations and without aeration $H_0$, as follows:

$$\varepsilon_e = 1 - \rho_b / \rho_a = 1 - H_0 / H \tag{12}$$

Secondly, we approach the analysis of the dust release at the bulk level according to Salehi *et al.* [40]. Accordingly, on the one hand the rate of released particles $N_p$ is proportional to the acceleration $a$ and to the frequency, $f$, of the mechanical vibrations. We have also to consider that, the dust particle release rate is inversely proportional to the interparticle attraction force, $F_c$:

$$N_p \propto fa\rho_p \frac{\pi d_{pw}^3}{6} \Big/ F_c \tag{13}$$

In this case the interparticle force $F_c$ can be related the powder tensile strength at low consolidation $\sigma_{t0}$ by means of the Rumpf equation [45]:

$$F_c = \sigma_{t0} d_p^2 \varepsilon_i / (1 - \varepsilon_i) \quad (14)$$

where $d_p$ is the Sauter mean particle size and $\varepsilon_i$ is the voidage internal to the aggregates, which can be derived from the aggregate density $\rho_a$ and the particle density $\rho_p$ :

$$\varepsilon_i = 1 - \rho_a / \rho_p \quad (15)$$

By combining Eqs (10) to (13) the following dimensionless relationship can be elaborated:

$$\chi = N_p \Big/ \left( \frac{A_t f a \rho_p \pi d_{pw}}{6 F_c} \right) \quad (16)$$

Barletta *et al*. [46] reported that the dynamic response of a vibrated fluidized bed can be compared to that of a pseudo homogeneous elastic column in which vibration propagate with a speed, $c$, and a viscous damping coefficient, $\gamma$. Experimental results suggested that the speed $c$ can be described by the equation proposed by Roy *et al*. [47] for fluidized beds:

$$c = \sqrt{E/\rho} = \sqrt{E_g / \varepsilon \rho} \quad (17)$$

where $E$ is the average bed elastic modulus, $E_g$ is the air elastic modulus and $\rho$ is the average density of the fluidized bed. In general, the elastic modulus relevant for sound propagation in air is that corresponding to an adiabatic volume change. However, Roy *et al*. [47] have demonstrated that the volume change due to a dynamic wave propagating in a fluidized bed is an isothermal process, because of the high heat capacity of the system. Accordingly, the bed elastic modulus can be assumed equal to the absolute gas pressure, $p \approx 100$ kPa, and, thus, the sound speed becomes:

$$c = \sqrt{\frac{p}{\varepsilon (1 - \varepsilon) \rho_p}} \quad (18)$$

Barletta *et al.* [46] have also proposed and verified experimentally an original expression for viscous damping coefficient, $\gamma$, described by:

$$\gamma \approx \frac{8cK\tan\phi_W}{\pi D_C} \tag{19}$$

where $\phi_w$ is the angle of wall friction and $K$ is the horizontal to vertical stress ratio that is a function of the effective angle of internal friction, $\phi_e$:

$$K = \frac{1-\sin\phi_e}{1+\sin\phi_e} \tag{20}$$

According to the model developed by Barletta *et al.* [46] the effective amplitude of the bed oscillation at the surface, $A(H)$, is related to the imparted oscillation amplitude, $A(0)$, by means of an amplitude ratio, $AR$:

$$AR = A(H)/A(0) = \sqrt{2}/\sqrt{\cos(2\beta H)+\cosh(2\delta H)} \tag{21}$$

where:

$$\delta = 2\pi\sqrt{\frac{-f^2+\sqrt{f^4+(\gamma f/2\pi)^2}}{2c^2}} \quad \text{and} \quad \beta = 2\pi\sqrt{\frac{f^2+\sqrt{f^4+(\gamma f/2\pi)^2}}{2c^2}} \tag{22}$$

this provides maxima of the amplitude ratio in correspondence of the system natural vibration frequencies given by

$$f_n = (2n+1)c/4H \quad \text{with} \quad n = 0, 1, 2, 3\ldots \tag{23}$$

At resonance frequencies the amplitude ratio shows a local peak value and the phase lag is close to $-\pi/2-n\pi$.

For sinusoidal vibrations the maximum acceleration, $a$, is proportional to the vibration amplitude, $A$, (i.e. half of the maximum vibration displacement) and to the second power of pulsation, $\omega$, which is related to the oscillation frequency, $f$:

$$a = A\omega^2 = A(2\pi f)^2 \tag{24}$$

Therefore, the proper acceleration to be used in Eq. (16) is

$$a = A(H)(2\pi f)^2 = AR\ A(0)(2\pi f)^2 \tag{25}$$

## 3. EXPERIMENTAL APPARATUS

A sketch of the experimental set up is reported in Figure 1. It is made of a vibrated fluidization column which also used by Salehi Kahrizsangi *et al*. [48] to fluidize powder. The vibrating column was coupled with a dust metering system.

### 3.1. Vibrated fluidization column

The fluidization column, (85 mm ID and 400 mm tall is made in perspex. Bed aeration is carried out with desiccated compressed air metered by two thermal mass flow controllers (Aera FC-7700C Aera, F and Tylan FC2900V) respectively providing a maximum flow rate of $1.7x10^{-5}$ $Nm^3 s^{-1}$ and $5x10^{-5}$ $Nm^3 s^{-1}$ (normal conditions at 0°C and atmospheric pressure). The air is fed to the column through a windbox and it is distributed by a porous plate made of 10 μm sintered brass spheres. The plate, 10 mm thick, is housed in the windbox flange connecting to the column. Pressure drops in the fluidized bed are measured with a water filled U-Tube manometer connected to a pressure port bored through the flange at the column bottom. The column with its windbox is hold by an aluminum and steel frame fixed to the vibrating plane of an electric inductance vibrator (V100 Gearing and Watson, USA). The vibrating plane moves in the vertical direction with a sinusoidal movement. The operating range of the vibrator allow movement frequencies between 2 and 6500 Hz and a maximum movement amplitudes of 12.7 mm. The maximum force that the system can apply to accelerate masses is of 26.7 kN. A piezoelectric accelerometer (8636B60M05 Kistler, USA) fixed on the metal frame transmits the controlling signal to the vibration controller connected to the amplifier. The controller, a model Sc-121 (Labworks inc., USA) is able to set vibration frequencies in the range between 2 and 6500 Hz.

### 3.2. Dust metering system

The dust was metered gravimetrically by the use of a paper filter with 300 nm porosity. In particular, the air in the bed freeboard is aspirated by a 40 mm ID tube connected to an air suction unit. Dust in this air stream is captured by a pouch of filter paper, which is fixed on the tube tip to minimize losses of dust adhering on the tube walls. The tube is hold vertically with the tip pointing downward and positioned some centimeters above the bed surface. The tube is hold steady and independently from the column movement in order to avoid to detachment and loss of the dust cake deposited in the filter surface.

## 4. MATERIAL AND METHODS

### 4.1. Materials characterization

Table 1 reports the properties of the two powders used in the experiments. These are a silica fine powder and a potato starch powder. A Schulze ring shear tester was used to characterize the powder flow properties [49]. The yield loci obtained at different consolidation provided the values of the cohesion, $C$, and of the angle of internal friction, $\phi_i$, of both powders as a function of the major consolidation. Cohesion is reported in Figure 2a, angle of internal friction in Figure 2b. It is assumed that the values relevant to fluidization, $C_0$ and $\phi_{i0}$, should correspond to zero consolidation. Therefore these values were obtained with an extrapolation procedure represented in Figure 2, by considering the intercepts of the data regression lines. Helium pycnometry by Quantachrome was used to measure the particle densities. The average bed density without vibration and the average vibrated powder density were obtained in fluidization experiments, without vibration and with vibration, respectively.

### 4.2. Fluidization

Both Silica and Potato Starch powders do not fluidize properly without vibrations. Typical fluidization curves for silica and potato starch powders are reported in Figure 3 which refer to a vibration acceleration at $a/g$=8 and to a vibration frequency of 70 Hz for Potato Starch and 120 Hz for Silica. The filled symbols and empty symbols refer to increasing and decreasing velocity experiments, respectively. It appears a rather smooth fluidization with maximum pressure drops different from what expected by non-vibrated fluidization and bed expansion which starts before the attainment of constant pressure drops due to the energy applied by vibrations. This peculiar phenomenology of vibrated powders fluidization was discussed by Barletta *et al*. [50]

### 4.3. Dust release

In the experiments dedicated to the dust release measurements, fluidization of Silica and Potato starch powders was carried out at two different gas flow rates of 2.12 $10^{-5}$ $Nm^3$ $s^{-1}$ and 1.94 $10^{-5}$ $Nm^3$ $s^{-1}$. The corresponding gas superficial velocities are 2.13 mm $s^{-1}$ and 3.74 mm $s^{-1}$. These provide good fluidization conditions for both powders. Acceleration of the imparted vibration were changed in a wide range. Expressing acceleration in terms of the vibration to gravity acceleration ratio, $a/g$, the range of acceleration explored is included between 5 and 9. The range of the tested frequencies spans between 50 and 150 Hz. The experiment were carried out by deliberately fixing vibration acceleration and frequency. The vibration amplitude is not independent and is related to acceleration and frequency by Eq. (24). The effective acceleration acting on the powder has to account also for the bed response and, therefore is given by Eq. (25). Bed masses were changed between 0.3 and 0.6 kg for Silica and between 0.225 and 0.450 for Potato Starch. These masses correspond for both materials to bed heights around 50 mm. Fluidization was smooth in most of the tested conditions apart from tests carried out close to the

natural vibration frequencies of the beds. The phenomenon of bed natural vibration is thoroughly examined by Barletta *et al*. [46] and will be more deeply discussed in the following.

The height of the suction tube above the bed surface was found to be 210 mm. In fact, a too low positioning of the suction tube tip would lead to the capture of material directly from the bed surface by the air flow induced by the air suction. Too high positioning of the suction probe would lead to an excessive accumulation of material on the freeboard walls, with the consequent impairing of the measured amount of the dust release. The most appropriate height for the suction probe was identified in a preliminary and dedicated set of experiments in a steady (not vibrated) and not aerated bed. In such conditions, the only mechanism for dust capture in the probe was determined by the surface air flow induced by suction. Therefore, the most appropriate height was identified as the lowest one at which the amount of captured dust was negligible.

In the experiments dedicated to the measure of dust emission, vibration aeration and air suction for dust capture were initiated at the same time. The air suction was generally carried out for 30 seconds, after which, the filter was taken out from the suction tube and weighed on the analytical balance to determine the amount of the captured dust. In some preliminary experiments, the possibility that an excess of dust could bring to the filter clogging and the consequent loss of measure consistency was excluded by verifying that the amount of collected solids changed linearly with the air suction time. All the dust emission measures are the results of an average over 10 repetitions. Significant electrostatics effects was excluded on the basis of no evidence of any related phenomena.

## 5. EXPERIMENTAL RESULTS

Different experiments were performed to highlight the effect of different process variables. Figure 4 reports the results of a first set of experiments in which the acceleration ratio was varied from 5 to 9. These experiments for each powder were conducted at two fixed frequency values, 120 Hz and 70 Hz. Each experimental condition was repeated at least 10 times. Averages and standard deviations are reported in In Figure 4 as data points and error bars. To minimize possible time related effects, such as long agglomeration or compaction the material was completely renovated between one testing condition and the other. Inspection of Figure 10 indicates that with increasing acceleration ratios also the amount of captured dust increases, for both powder. At 70 Hz, the amount of the emitted dust from both powders were similar. Also at 120 Hz, for the two powders similar amounts of dust weights were captured, but these values were much smaller than at 70 Hz. Clearly visible bubbling phenomena were observed at frequency of 70 Hz and acceleration ratio of more than 7. Correspondingly significantly higher amount of dust were collected.

The fact that the frequency is significant to the results appears clearly in Figure 4. For deeper investigation on the effect of frequency on captured dust, a new set of experiments were performed by setting acceleration ratio, $a/g$, at 7 and changing the frequency between 25 Hz and 150 Hz. For each material two different bed masses were tested, namely 0.3 and 0.6 kg for Silica and 0.225 and 0.450 for Potato Starch. Results are reported in Figure 5. For Silica with the bed mass of 0.3 kg, 70 Hz was the lowest frequency tested due to the observed intense bed surface oscillation at lower frequencies that made the measurement impossible. According to Eq. (24), lower frequencies correspond to larger vibration amplitudes, by keeping the acceleration constant.

Figure 5a and 5b report the amount of released dust for Silica powder and Potato Starch at different bed masses respectively. In general, increasing the frequency determines a reduction in the amount of released dust for both powders, independently of the bed mass. Inspecting Figure 5, reveals a maximum released dust amounts at about 100 Hz for the 0.6 kg Silica bed, at about 80 Hz for the 0.225 kg Potato Starch bed and at about 120 Hz for the 0.450 kg Potato Starch bed. These observations can also be matched with the observed intense bed surface oscillation below 70 Hz and 50 Hz for the 0.3 kg Silica bed and for the 0.450 kg Potato Starch bed respectively. These frequencies can find close matching with the natural bed resonance frequencies introduced above. The principal resonance frequencies, calculated according to Eq. (23) for the tested beds are reported in Figure 5. It appears that the frequency of the first resonance harmonic ($n$=0), assessed at the highest bed expansion, of silica powder with a bed mass of 0.3 kg is approximately 48 Hz, while it is 84 Hz for the 0.225 kg potato starch .

As reported by Barletta and Poletto [37] a clear relationship exists between the resonance conditions and the quality of fluidization. In fact, also in the systems observed in this paper there is a strict relationship between the conditions of natural resonance of the bed bubbling. Due to the intense bubbling, the bed behavior becomes too chaotic when approaching the bed resonance. Therefore it was not possible to have reliable data of dust release too close to the bed natural oscillation frequencies.

For better understanding the of frequency effect on dust generation, other experimental setup were carried out with different bed masses and different frequencies Figure 6a and 6b reports released dust results for both Silica and Potato Starch powders at different frequency, bed mass and acceleration ratio. Natural frequencies and bed masses are reported in Table 2. In these experiments, tests with different bed masses were coupled with the vibration frequencies in a

way that the ratio between the applied frequency, $f$, and the main resonance frequencies, $f_0$, are kept constant in the couple. These couples are represented by symbols with the same shapes. For each couple, the filled symbol is used to represent the results obtained from the smaller bed mass and the empty symbol to represent results obtained from the larger bed mass.

As it can be observed from Figure 6, by comparing filled symbols with empty symbols having the same shape, beds characterized by different bed heights but similar frequency ratios, $f/f_0$, are characterized by significantly different masses of the released dust.

In order to verify if it is possible to find a general dependency of the dust release rate with frequency, Figure 7 shows all the dust release data as a function of tested frequency. No specific trend can be detected in the untreated data and also the largest release rates are found for frequencies between 20 and 80 Hz.

## 6. DISCUSSION

The calculation procedure of the dimensionless parameter $\chi$ should account for several phenomena affecting the released dust amounts. These phenomena are mostly governed by the material cohesion that determines the self-aggregation of powder, which in turn affects both the overall surface of material releasing dust and also the force necessary to release a single dust grain. Vibration is accounted for 3 effects on dust release. First, its effect at the aggregate level to determine its size, second at the particle level to promote dust release and finally at the macroscopic level to vibrate the whole bed. In particular, taking into account the amplitude ratio, $AR$, described by Eq. (21) in the calculation of $\chi$, Eq. (16), it is possible to obtain a $\chi$ value which includes the effective oscillation of the system and not the imparted oscillation.

Table 3 reports the experimental conditions and the values of $\chi$ for all the experiments reported in Figure 4. Table 3 also reports the aggregates surface area, $A_t$ (11), the average dust particle

connecting force, $F_c$ (14), the dust particle number release rate, $N_p$ (13) and $\chi$ (16). In these equations $H_b$ is the bed height at fluidization and vibration, $H_{b0}$ is the initial bed height and $W_d$ is the dust release mass rate.

Inspection of table three shows that for the same material and vibration frequency the parameter $\chi$ is only slightly affected by acceleration changes. Also the values of $\chi$ for the two different materials at the same frequency are found if we exclude intense bubbling results for Silica at acceleration ratios larger than 7. This result is noteworthy considering that The attraction force at the contacts between particles and aggregate $F_c$ are calculated from Eq. (14) considering the bulk flow properties and the evaluation does not involve any fitting parameter. On the other hand the use of powder flow properties to evaluate $F_c$, indirectly includes the effect of specific particle properties such as hardness and shape. In spite of the good performace of the parameter $\chi$ to account for changing acceleration ratios and material properties, it has to be considered the fact that the effect of frequency is not fully caught by this parameter.

These variations due to frequency might suggest the occurrence of other mechanisms than simply the energy transfer affected by vibration frequency. An effect that was not considered in our model and may play a significant role to be considered is the ability of the upper layer to effectively recapture dust under the effect of vibrations [25].

Independently from the specific mechanisms explaining the strong frequency effect, it can be of interest to verify if the frequency dependence of the release rate is better correlated in terms of the dimensionless parameter $\chi$ rather than in terms of the mass release rate as shown in Figure 7. To verify this, Figure 8 reports the parameter $\chi$ as function of the tested frequencies. Inspection of this Figure indicates that inclusion of the effective acceleration in the expression of $\chi$ only partly improve the correlation. The representation of data in terms of $\chi$, in fact, does not

compensate for the general increase of dust release at the lowest frequencies. Furthermore, at intermediate frequencies, there are conditions in which the values of $\chi$ shows local maxima. Perhaps the expression of $\chi$ is not able to fully compensate the increased system oscillations close to the bed natural frequencies. In order to verify this, in Figure 9 the parameter $\chi$ is plotted as a function of the frequency normalized to the frequency of the first bed harmonic. In this representation, natural bed resonances should occur for frequencies close to 1 and to 3 of this ratio. Inspection of Figure 9 indicates very similar trends obtained with the two materials, especially at low frequencies. Both materials show some deviation at values of $f/f_0$ close to 1.3 and 2.2. These values do not exactly correspond to the natural frequency values but it can be verified that the local maxima in $\chi$ correspond to tests providing intense bubbling conditions. When bubbling occurs, the dust release mechanism is completely different than the hypothesized one at the basis of the definition of $\chi$. Figure 9 shows that a power law curve can fit the data following the general reduction trend of the release rate with the frequency.

## 7. CONCLUSIONS

Dust release from powders has been assessed by employing an experimental method based on vibrated fluidized bed. This set up is made of a vibrated bed in which it is possible to adjust vibration acceleration, frequency and to fix a crossing gas flow rate.

In general, the experimental trends of the dust release indicate a favorable effect of the system acceleration and a considerable reduction of the dust emission rates at the highest frequencies. The largest release rates are found for frequencies between 20 and 80 Hz. Higher dust release rates, in terms of mass, are found with potato starch than with silica.

The impact of process condition on dust emission has been analyzed in the light of a theoretical model. A dimensionless dust release parameter, $\chi$, has been defined and calculated

from the experimental results. The developed approach shows that the dimensionless dust release parameter $\chi$ is able to catch most of the significant effects of both acceleration and material cohesion on dust emission also accounting for the magnification effects of acceleration intensity close to resonance conditions. The parameter $\chi$, however, fails to correctly predict direct and indirect effect of vibration frequency.

Dedicated sets of experiments have been carried out to verify the effect of vibration in terms of frequency and acceleration ratio. In addition, the effect of bed mass on dust release has been studied. A strong non-monotonic dependence of $\chi$ on the frequency is found. Plotting the values of the parameter $\chi$ as a function of the dimensional frequency suggests that, in spite of what has been considered in $\chi$ definition, this parameter is not able to fully account for the bed resonance effects. Dust recapture in the bed upper layers may play a role that should be further investigated, which might take a significant role in dust release rate from the bed.

Still a great amount of work has to be done to be able to relate experimental results at the lab scale to practical cases in the field. However, we believe that a proper link between the lab scale of these experiments and the real scale of application of industrial interest for dust release of vibrated powders, such as in the case of vibration applied by transport systems, may come only from a proper understanding of the fundamental phenomena occurring in the systems. The understanding includes also the role of the agglomerate mesoscale typical of the aggregates formed by cohesive powders. Similar experiments such as those carried out in this paper may as well verify the effectiveness of some of the major strategies used to fight dust release, such as the use of humidity to increase powder cohesion and, therefore, the forces binding dust particles to aggregates of non entrainable size.

## LIST OF SYMBOLS

| | |
|---|---|
| $a$ | acceleration due to vibration, m $s^{-2}$ |
| $A$ | vibration amplitude, m |
| $A(0)$ | imparted oscillation amplitude, |
| $A(H)$ | effective amplitude of the bed oscillation at the surface, |
| $AR$ | amplitude ratio, |
| $C$ | cohesion, Pa |
| $c$ | sound speed, m $s^{-1}$ |
| $C_0$ | cohesion extrapolated to zero consolidation, Pa |
| $d_a$ | aggregate diameter, m |
| $d_p$ | particle diameter, m |
| $d_{pw}$ | volumetric average of particle diameter, $m^3$ |
| $E$ | average bed elastic modulus, Pa |
| $E_g$ | elastic modulus of the air, Pa |
| $f$ | frequency, $s^{-1}$ |
| $F_c$ | attraction force at the contacts between the aggregate and the upper lumps of the solids, N |
| $f_i$ | resonance frequencies, $s^{-1}$ |
| $g$ | acceleration due to gravity, m $s^{-2}$ |
| $k$ | effective number of contacts between an aggregate and another layer, - |
| $K$ | the horizontal to vertical stress ratio, - |
| $H$ | bed height, m |
| $H_0$ | initial bed height, m |
| $H_b$ | bed height at the minimum for bubbling, m |

$H_b$ bed height at the maximum for channeling, m

$i$ vibration modes, -

ID internal diameter, m

$m_b$ bed mass, kg

$n_c$ contact density between aggregates in neighboring layers, -

$W_d$ dust release mass rate, kg $s^{-1}$

$N_p$ dust particle number release rate, $s^{-1}$

$p$ gas pressure, Pa

**Greek symbols**

$\varepsilon$ average bed voidage, -

$\varepsilon_i$ voidage internal to aggregates, -

$\varepsilon_e$ voidage external to the aggregates, -

$\beta$ parameter in Eqs (21) and (22), -

$\delta$ parameter in Eqs (21) and (22), -

$\rho$ average density of the fluidized bed, kg $m^{-}$

$\rho_a$ aggregate density, kg $m^{-3}$

$\rho_b$ average bed density, kg $m^{-3}$

$\rho_{b0}$ average bed density without vibration, kg $m^{-3}$

$\rho_p$ particle density, kg $m^{-3}$

$\sigma$ normal stress, Pa

$\sigma_1$ major principal stress at consolidation, Pa

$\sigma_t$ tensile strength, Pa

$\sigma_{t0}$ tensile strength at zero consolidation, Pa

$\Sigma_c$ column cross section, $m^2$

$\tau$ shear stress, Pa

$\phi_i$ angle of internal friction, deg

$\phi_{i0}$ angle of internal friction extrapolated to zero consolidation, deg

$\phi_w$ angle of wall friction, deg

$\chi$ dimensionless dust release parameter, -

$\omega$ proportional pulsation value, $s^{-1}$

$\gamma$ viscous damping coefficient, N s $m^{-1}$

## REFERENCES

(1) Kilbane-Dawe, I.; Clement, L. *The Impacts of Air Pollution on Health: A Summary of the State of Current Knowledge*; London, UK, 2014.

(2) Wypych, P. W. Dust Explosion Hazard Considerations for Materials Handling Plants. In *Handbook of Powder Technology*; Levy, A., Kalman, H., Eds.; Handbook of Powder Technology; Elsevier: Amsterdam, NL, 2001; Vol. 10, pp 745–752.

(3) Morgeneyer, M.; Le Bihan, O.; Ustache, A.; Aguerre-Chariol, O. Experimental Study of the Aerosolization of Fine Alumina Particles from Bulk by a Vortex Shaker. *Powder Technol.* **2013**, *246*, 583–589.

(4) Wangchai, S.; Hastie, D. B.; Wypych, P. W. The Investigation of Particle Flow Mechanisms of Bulk Materials in Dustiness Testers. *Part. Sci. Technol.* **2015**, *34*, 241–254.

(5) Ansart, R.; Ryck, A. de; Dodds, J. A. Dust Emission in Powder Handling: Free Falling Particle Plume Characterisation. *Chem. Eng. J.* **2009**, *152*, 415–420.

(6) Ansart, R.; de Ryck, A.; Dodds, J. A.; Roudet, M.; Fabre, D.; Charru, F. Dust Emission by Powder Handling: Comparison between Numerical Analysis and Experimental Results. *Powder Technol.* **2009**, *190*, 274–281.

(7) Shandilya, N.; Le Bihan, O.; Morgeneyer, M. A Review on the Study of the Generation of (Nano)particles Aerosols during the Mechanical Solicitation of Materials. *J. Nanomater.* **2014**, *2014*, 1–16.

(8) Ansart, R.; Letourneau, J.-J.; de Ryck, A.; Dodds, J. A. Dust Emission by Powder Handling: Influence of the Hopper Outlet on the Dust Plume. *Powder Technol.* **2011**, *212*, 418–424.

(9) Faschingleitner, J.; Höflinger, W. Evaluation of Primary and Secondary Fugitive Dust Suppression Methods Using Enclosed Water Spraying Systems at Bulk Solids Handling. *Adv. Powder Technol.* **2011**, *22*, 236–244.

(10) Hamelmann, F.; Schmidt, E. Methods for Characterizing the Dustiness Estimation of Powders. *Chem. Eng. Technol.* **2004**, *27*, 844–847.

(11) Wypych, P.; Cook, D.; Cooper, P. Controlling Dust Emissions and Explosion Hazards in Powder Handling Plants. *Chem. Eng. Process.* **2005**, *44*, 323–326.

(12) Saleh, K.; Moufarej Abou Jaoude, M.-T.; Morgeneyer, M.; Lefrancois, E.; Le Bihan, O.; Bouillard, J. Dust Generation from Powders: A Characterization Test Based on Stirred Fluidization. *Powder Technol.* **2014**, *255*, 141–148.

(13) Le Bihan, O. L. C.; Ustache, A.; Bernard, D.; Aguerre-Chariol, O.; Morgeneyer, M. Experimental Study of the Aerosolization from a Carbon Nanotube Bulk by a Vortex Shaker. *J. Nanomater.* **2014**, *2014*, 1–11.

(14) Shandilya, N.; Morgeneyer, M.; Le Bihan, O. First Development to Model Aerosol

Emission from Solid Surfaces Subjected to Mechanical Stresses: I. Development and Results. *J. Aerosol Sci.* **2015**, *89*, 43–57.

(15) Shandilya, N.; Morgeneyer, M.; Bihan, O. Le. First Development to Model Aerosol Emission from Solid Surfaces Subjected to Mechanical Stresses: II. Experiment-Theory Comparison, Simulation and Sensibility Analysis. *J. Aerosol Sci.* **2015**, *89*, 1–17.

(16) Gupta, R.; Mujumdar, A. S. Aerodynamics of a Vibrated Fluid Bed. *Can. J. Chem. Eng.* **1980**, *58*, 332–338.

(17) Morse, R. D. Sonic Energy in Granular Solid Fluidization. *Ind. Eng. Chem.* **1955**, *47*, 1170–1175.

(18) Zhu, C.; Liu, G.; Yu, Q.; Pfeffer, R.; Dave, R. N.; Nam, C. H. Sound Assisted Fluidization of Nanoparticle Agglomerates. *Powder Technol.* **2004**, *141*, 119–123.

(19) Guo, Q.; Liu, H.; Shen, W.; Yan, X.; Jia, R. Influence of Sound Wave Characteristics on Fluidization Behaviors of Ultrafine Particles. *Chem. Eng. J.* **2006**, *119*, 1–9.

(20) Xu, C.; Cheng, Y.; Zhu, J. Fluidization of Fine Particles in a Sound Field and Identification of Group C/A Particles Using Acoustic Waves. *Powder Technol.* **2006**, *161*, 227–234.

(21) Levy, E. K.; Celeste, B. Combined Effects of Mechanical and Acoustic Vibrations on Fluidization of Cohesive Powders. *Powder Technol.* **2006**, *163*, 41–50.

(22) Chirone, R.; Massimilla, L.; Russo, S. Bubble-Free Fluidization of a Cohesive Powder in an Acoustic Field. *Chem. Eng. Sci.* **1993**, *48*, 41–52.

(23) Russo, P.; Chirone, R.; Massimilla, L.; Russo, S. The Influence of the Frequency of Acoustic Waves on Sound-Assisted Fluidization of Beds of Fine Particles. *Powder Technol.* **1995**, *82*, 219–230.

(24) Urciuolo, M.; Salatino, P.; Cammarota, A.; Chirone, R. Development of a Sound-Assisted Fluidized Bed Filter/afterburner for Particle-Laden Gas Clean-Up. *Powder Technol.* **2008**, *180*, 102–108.

(25) Chirone, R.; Urciuolo, M. Role of Bed Height and Amount of Dust on the Efficiency of Sound-Assisted Fluidized Bed Filter/afterburner. *AIChE J.* **2009**, *55*, 3066–3075.

(26) Ammendola, P.; Chirone, R.; Raganati, F. Effect of Mixture Composition, Nanoparticle Density and Sound Intensity on Mixing Quality of Nanopowders. *Chem. Eng. Process.* **2011**, *50*, 885–891.

(27) Ammendola, P.; Chirone, R.; Raganati, F. Fluidization of Binary Mixtures of Nanoparticles under the Effect of Acoustic Fields. *Adv. Powder Technol.* **2011**, *22*, 174–183.

(28) Marring, E.; Hoffmann, A. C.; Janssen, L. P. B. M. The Effect of Vibration on the Fluidization Behaviour of Some Cohesive Powders. *Powder Technol.* **1994**, *79*, 1–10.

(29) Janssen, L. P. B. M.; Marring, E.; Hoogerbrugge, J. C.; Hoffmann, A. C. The Mechanical Behaviour of Vibrated, Aerated Beds of Glass and Starch Powder. *Chem. Eng. Sci.* **1998**, *53*, 761–772.

(30) Xu, C.; Zhu, J. Experimental and Theoretical Study on the Agglomeration Arising from Fluidization of Cohesive Particles - Effects of Mechanical Vibration. *Chem. Eng. Sci.* **2005**, *60*, 6529–6541.

(31) Xu, C.; Zhu, J. Parametric Study of Fine Particle Fluidization under Mechanical Vibration. *Powder Technol.* **2006**, *161*, 135–144.

(32) Valverde, J. M.; Castellanos, A. Effect of Vibration on Agglomerate Particulate Fluidization. *AIChE J.* **2006**, *52*, 1705–1714.

(33) Valverde, J. M.; Castellanos, A. Fluidization, Bubbling and Jamming of Nanoparticle Agglomerates. *Chem. Eng. Sci.* **2007**, *62*, 6947–6956.

(34) Liang, X.; Duan, H.; Wang, J.; Zhou, T. Agglomerating Vibro-Fluidization Behavior of Binary Nanoparticles Mixtures. *Procedia Eng.* **2015**, *102*, 887–892.

(35) Liang, X.; Zhou, Y.; Zou, L.; Kong, J.; Wang, J.; Zhou, T. Fluidization Behavior of Binary Iron-Containing Nanoparticle Mixtures in a Vibro-Fluidized Bed. *Powder Technol.* **2016**, *304*, 101–107.

(36) Mawatari, Y.; Hamada, Y.; Yamamura, M.; Kage, H. Flow Pattern Transition of Fine Cohesive Powders in a Gas-Solid Fluidized Bed under Mechanical Vibrating Conditions. *Procedia Eng.* **2015**, *102*, 945–951.

(37) Barletta, D.; Poletto, M. Aggregation Phenomena in Fluidization of Cohesive Powders Assisted by Mechanical Vibrations. *Powder Technol.* **2012**, *225*, 93–100.

(38) Yin, S.; Tang, W.; Zheng, X.; Tong, L.; Wang, L.; Liu, C. Entrainment Characteristics of Fine Particles in Fluidized Bed under Preheating Conditions. *Powder Technol.* **2016**, *299*, 150–155.

(39) Barletta, D.; Donsì, G.; Ferrari, G.; Poletto, M.; Russo, P. Solid Flow Rate Prediction in Silo Discharge of Aerated Cohesive Powders. *AIChE J.* **2007**, *53*, 2240–2253.

(40) Salehi Kahrizsangi, H.; Sofia, D.; Barletta, D.; Poletto, M. Dust Generation in Vibrated Cohesive Powders. *Chem. Eng. Trans.* **2015**, *43*, 769–774.

(41) Rumpf, H. *The Strength of Granules and Agglomerates*; Knepper, W., Ed.; Wiley: New York, 1962.

(42) Kendall, K.; Alford, N. M.; Birchall, J. D. Elasticity of Particle Assemblies as a Measure of the Surface Energy of Solids. *Proc. R. Soc. A Math. Phys. Eng. Sci.* **1987**, *412*, 269–

283.

(43) Kim, J.; Han, G. Y. Effect of Agitation on Fluidization Characteristics of Fine Particles in a Fluidized Bed. *Powder Technol.* **2006**, *166*, 113–122.

(44) Zhou, T.; Li, H. Estimation of Agglomerate Size for Cohesive Particles during Fluidization. *Powder Technol.* **1999**, *101*, 57–62.

(45) Rumpf, H. C. H. Zur Theorie Der Zugfestigkeit von Agglomeraten Bei Kraftübertragung an Kontaktpunkten. *Chem. Ing. Tech.* **1970**, *42*, 538–540.

(46) Barletta, D.; Russo, P.; Poletto, M. Dynamic Response of a Vibrated Fluidized Bed of Fine and Cohesive Powders. *Powder Technol.* **2013**, *237*, 276–285.

(47) Roy, R.; Davidson, J. F.; Tuponogov, V. G. The Velocity of Sound in Fluidised Beds. *Chem. Eng. Sci.* **1990**, *45*, 3233–3245.

(48) Kahrizsangi, H. S.; Barletta, D.; Poletto, M. Mechanical Properties of Agglomerates Produced by the Mechanical Vibration of Cohesive Powders. *KONA Powder Part. J.* **2016**, *33*, 287–295.

(49) Salehi, H.; Barletta, D.; Poletto, M. A Comparison between Powder Flow Property Testers. *Particuology* **2017**, *32*, 10–20.

(50) Barletta, D.; Donsì, G.; Ferrari, G.; Poletto, M.; Russo, P. The Effect of Mechanical Vibration on Gas Fluidization of a Fine Aeratable Powder. *Chem. Eng. Res. Des.* **2008**, *86*, 359–369.

## FIGURE CAPTIONS

**Figure 1.** Experimental apparatus. 1, Aerated column; 2, vibrating stand; 3, Frame; 4, Air feed control; 5, accelerometer; 6, U tube manometer; 7, Vibration controlling and actuating unit; 8, Suction probe; 9, filter pouch; 10, Suction unit; 11, holder of the suction probe.

**Figure 2.** Powder cohesion (a) and angle of internal friction (b) reported as a function of the major consolidation stress. These values were evaluated from the powder yield loci measured with the Schulze ring shear tester. Lines and equations are best fit linear regressions.

**Figure 3.** Bed expansion (a and b) and fluidization (c and d) curves at a/g=8. a) and c) 0.300 kg Silica bed mass at 120 Hz; b) and d) 0.255 kg Potato Starch bed mass at 70 Hz..

**Figure 4.** Released dust for silica and potato starch at different acceleration ratios between 5 to 9 at a) frequency of 70 Hz and b) frequency of 120 Hz.

**Figure 5.** Effect of bed mass on released dust at fixed acceleration ratio of $a/g$=7 and different frequencies between 50 Hz and 150 Hz. a) Silica and b) Potato starch. Vertical lines correspond to frequencies of bed harmonics as described.

**Figure 6.** Effect of bed mass and frequency on captured dust at different acceleration ratio, for Silica and Potato starch.

**Figure 7.** All the data obtained for dust release plotted as a function of the vibration frequency.

**Figure 8.** Dimensionless dust release rate $\chi$ reported as a function of the vibration frequency for a) Silica and b) Potato Starch.

**Figure 9.** Dimensionless dust release rate $\chi$ reported as a function of the normalized frequency $f/f_0$ for both Silica and Potato Starch.

## TABLE CAPTIONS

**Table 1.** Materials properties

**Table 2.** Bed mass and main frequency values for beds in Figure 6.

**Table 3.** Model estimates for silica and potato starch powders at two different frequencies and different acceleration ratio.

**Table 1.** Materials properties

| *Material* | $d_p$ µm | $d_{p10}$ µm | $d_{p50}$ µm | $d_{p90}$ µm | $\rho_p$ kg m$^{-3}$ | $\rho_{bv}$ kg m$^{-3}$ | $\rho_{b0}$ kg m$^{-3}$ | $C_{i0}$ Pa | $\phi_{i0}$ deg | $\sigma_{t0}$ Pa |
|---|---|---|---|---|---|---|---|---|---|---|
| Silica | 7.6 | 2.8 | 21 | 66 | 2650 | 1400 | 1020 | 43.3 | 36.7 | 43.4 |
| Potato starch | 21 | 23 | 46 | 80 | 1570 | 854 | 773 | 24.2 | 25.3 | 30.7 |

**Table 2.** Bed mass and main frequency values for beds in Figure 6.

| Material | bed mass (g) | bed height (mm) | $f_0$ (hz) | $f_1$ (hz) |
|---|---|---|---|---|
| **Silica** | 300 | 48 | 48 | 144 |
| **Silica** | 514 | 89 | 35 | 106 |
| **Silica** | 600 | 96 | 24 | 72 |
| **Potato starch** | 225 | 45 | 84 | 252 |
| **Potato starch** | 385 | 90 | 41 | 122 |
| **Potato starch** | 450 | 90 | 42 | 126 |

**Table 3.** Model estimates for silica and potato starch powders at two different frequencies and different acceleration ratio.

| Materials | $f$(Hz) | $a/g$ | $H_b$(mm) | $H_{b0}$(mm) | $w_d$(μg.s$^{-1}$) | $A_t$, m$^2$ | $N_p$*10$^5$(s$^{-1}$) | Fc(nN) | $\chi$ 10$^{-9}$(-) |
|---|---|---|---|---|---|---|---|---|---|
| Silica | 70 | 5 | 60 | 48 | 4.41 | 7.92 | 3.43 | 3.50 | 230.29 |
| | | 6 | 60 | 48 | 7.55 | 9.95 | 5.88 | 3.50 | 273.94 |
| | | 7 | 60 | 48 | 12.04 | 11.26 | 9.37 | 3.50 | 320.80 |
| | | 8 | 60 | 48 | 24.68 | 12.67 | 19.2 | 3.50 | 503.54* |
| | | 9 | 60 | 48 | 65.12 | 14.25 | 50.7 | 3.50 | 1049.80* |
| | 120 | 5 | 60 | 48 | 0.40 | 7.92 | 0.30 | 3.50 | 24.58 |
| | | 6 | 60 | 48 | 0.42 | 9.95 | 0.32 | 3.50 | 18.13 |
| | | 7 | 60 | 48 | 0.58 | 11.26 | 0.45 | 3.50 | 18.57 |
| | | 8 | 60 | 48 | 0.67 | 12.67 | 0.53 | 3.50 | 16.60 |
| | | 9 | 60 | 48 | 0.86 | 14.25 | 0.67 | 3.50 | 16.81 |
| Potato Starch | 70 | 5 | 55 | 45 | 5.3 | 3.02 | 0.67 | 10.6 | 32.63 |
| | | 6 | 55 | 45 | 10.1 | 3.49 | 1.26 | 10.6 | 42.87 |
| | | 7 | 55 | 45 | 16.7 | 3.99 | 2.09 | 10.6 | 52.22 |
| | | 8 | 55 | 45 | 17.9 | 4.48 | 2.23 | 10.6 | 42.79 |
| | | 9 | 55 | 45 | 20.6 | 4.98 | 2.57 | 10.6 | 38.98 |
| | 120 | 5 | 55 | 45 | 1.0 | 3.02 | 0.12 | 10.6 | 31.07 |
| | | 6 | 55 | 45 | 0.4 | 3.49 | 0.05 | 10.6 | 8.95 |
| | | 7 | 55 | 45 | 0.4 | 3.99 | 0.04 | 10.6 | 5.67 |
| | | 8 | 55 | 45 | 0.3 | 4.48 | 0.04 | 10.6 | 4.11 |
| | | 9 | 55 | 45 | 0.8 | 4.98 | 0.10 | 10.6 | 7.61 |

*Bubbling condition

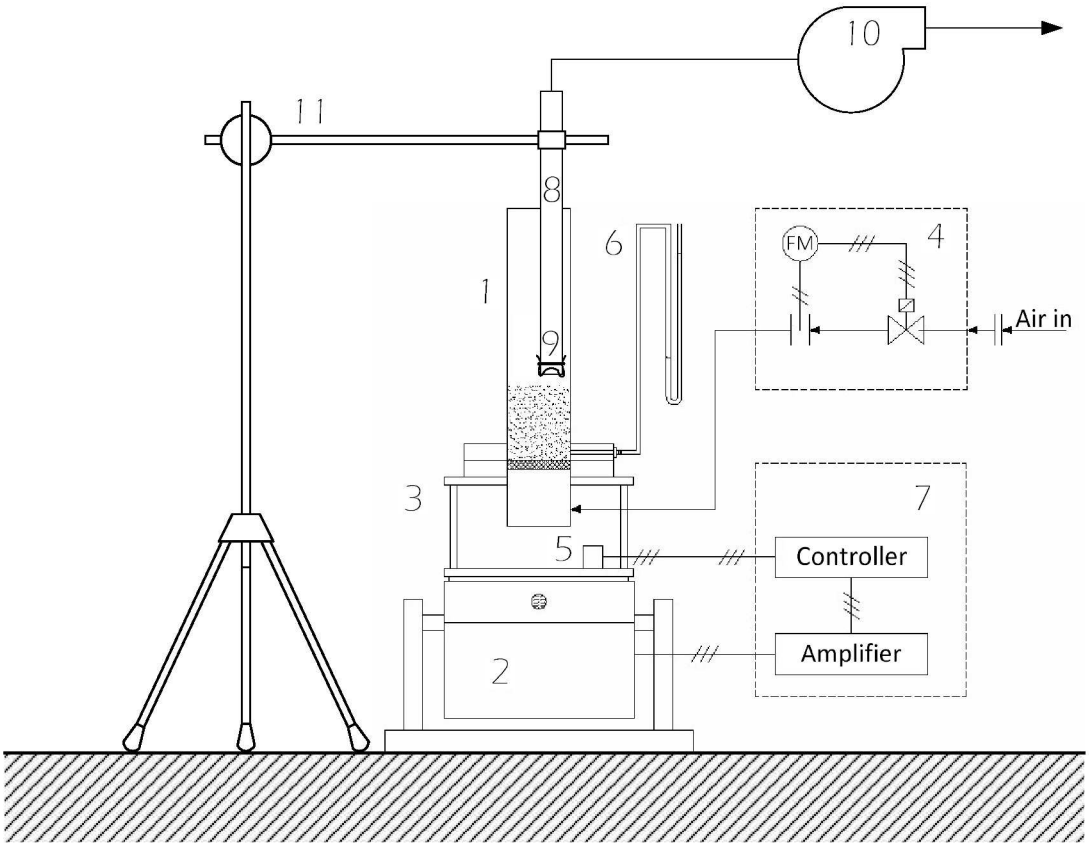


Figure 1. Experimental apparatus: 1, Aerated column; 2, vibrating stand; 3, Frame; 4, Air feed control; 5, accelerometer; 6, U tube manometer; 7, Vibration controlling and actuating unit; 8, Suction probe; 9, filter pouch; 10, Suction unit; 11, holder of the suction probe.

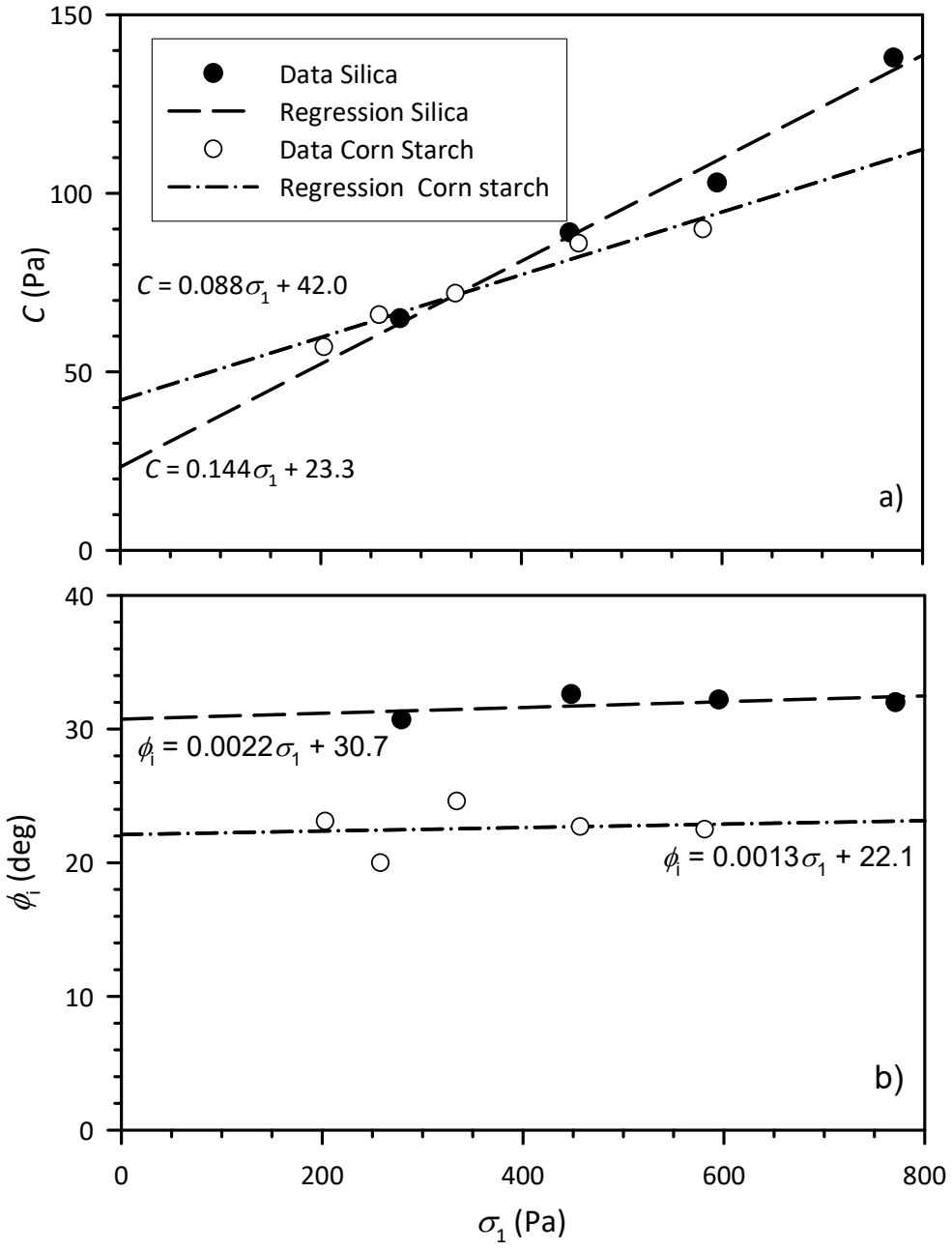


Figure 2. Powder cohesion (a) and angle of internal friction (b) reported as a function of the major consolidation stress. These values were evaluated from the powder yield loci measured with the Schulze ring shear tester: Lines and equations are best fit linear regressions.

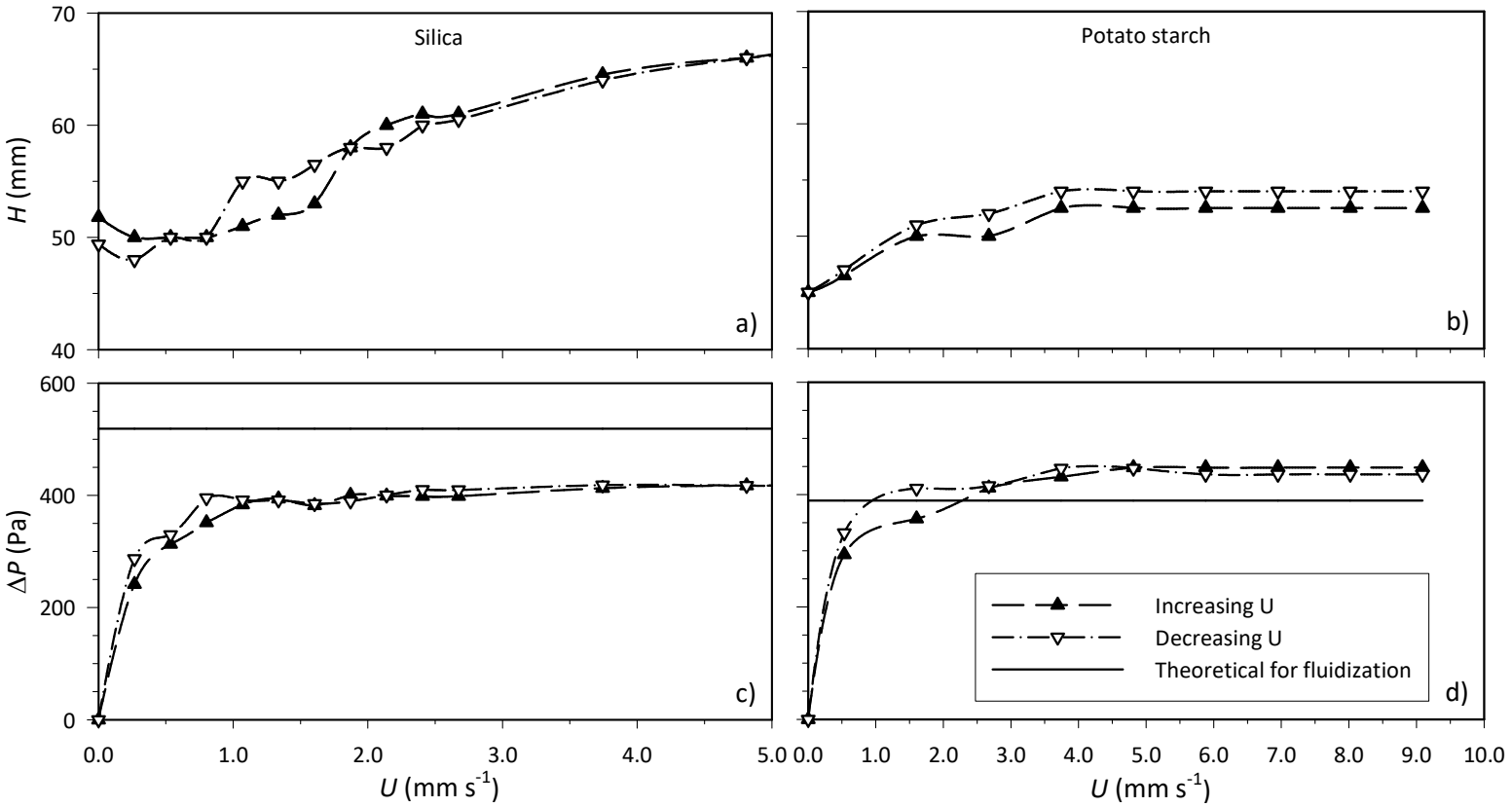


Figure 3. Bed expansion (a and b) and fluidization (c and d) curves at a/g=8. a) and c) 0.300 kg Silica bed mass at 120 Hz; b) and d) 0.255 kg Potato Starch bed mass at 70 Hz.

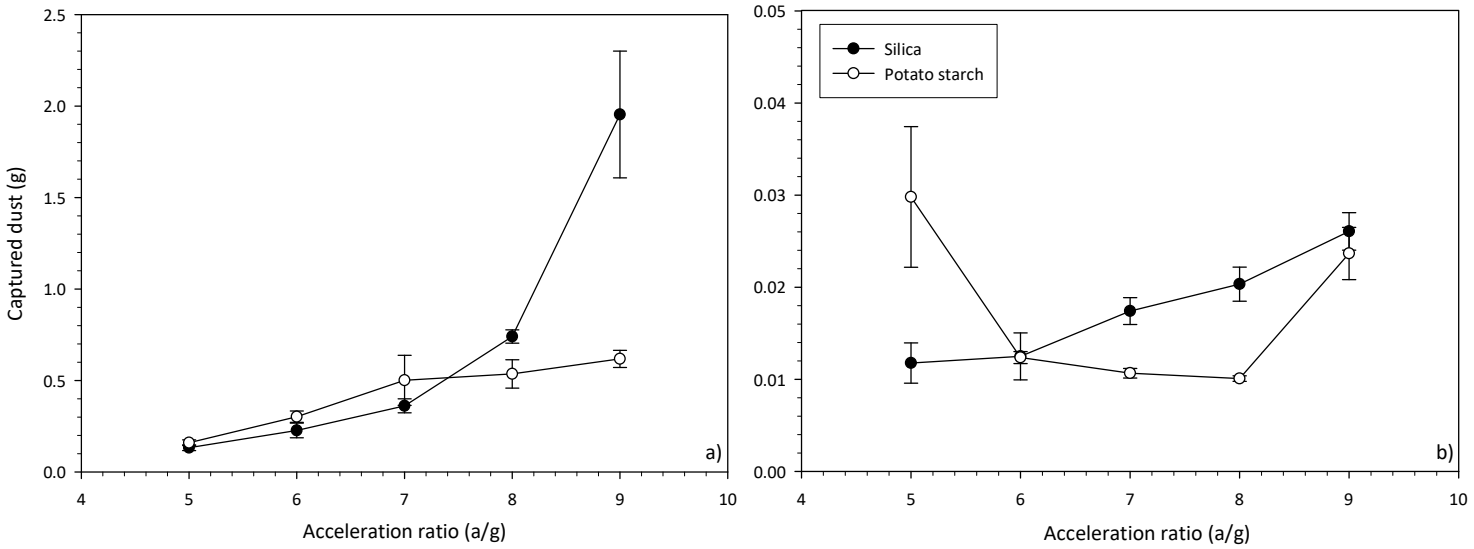


Figure 4. Released dust for silica and potato starch at different acceleration ratios between 5 to 9 a) frequency of 70 Hz and b) frequency of 120 Hz.

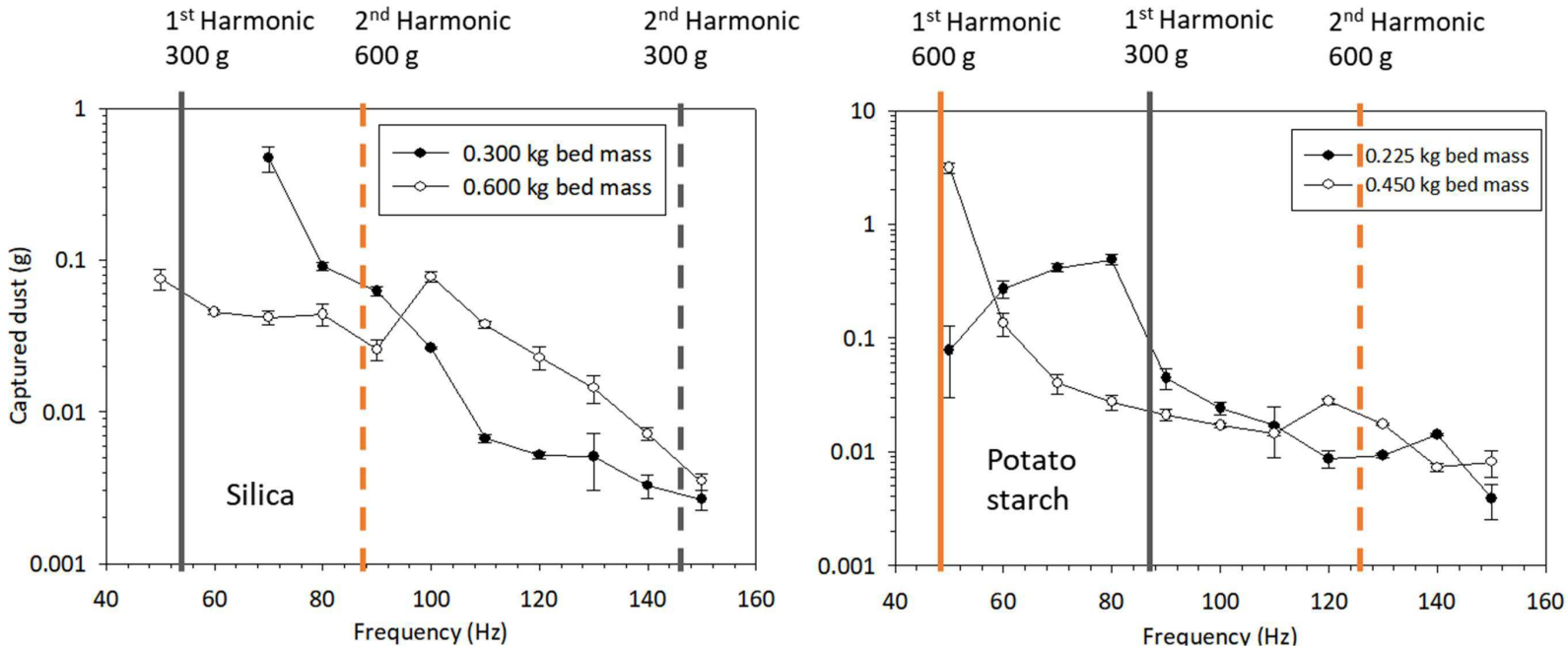


Figure 5. Effect of bed mass on released dust at fixed acceleration ratio of $a/g$=7 and different frequencies between 50 Hz and 150 Hz. a) Silica and b) Potato starch. Vertical lines correspond to frequencies of bed harmonics as described.

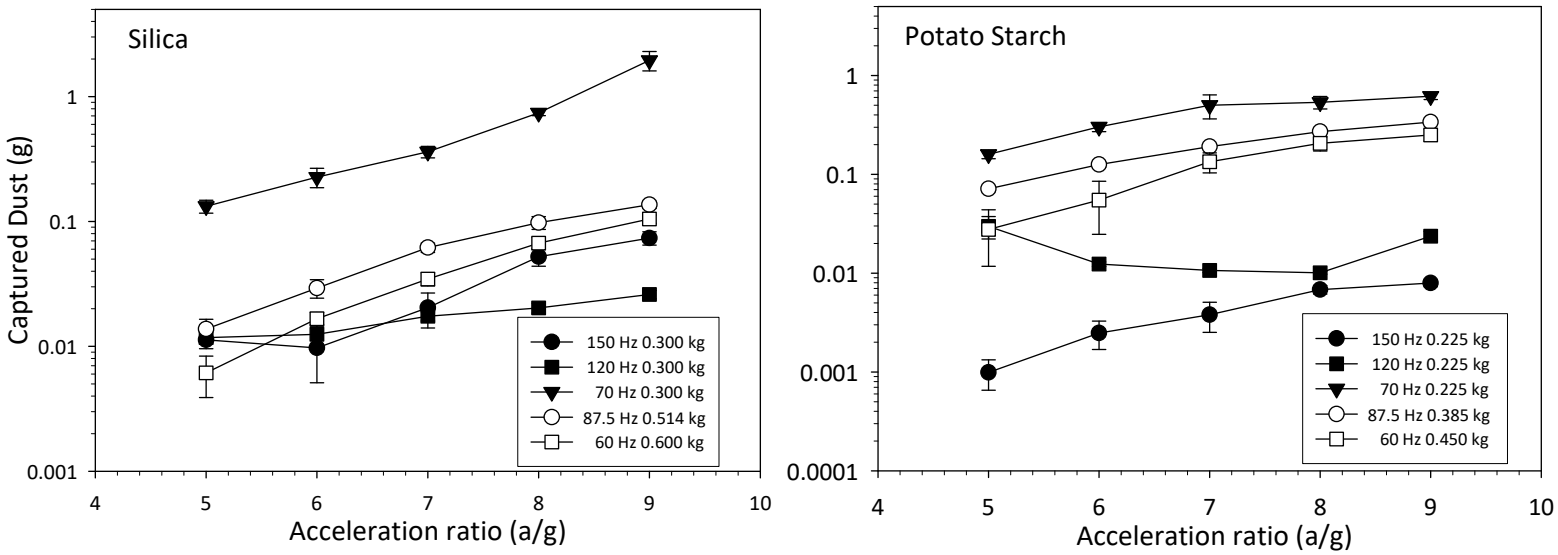


Figure 6. Effect of bed mass and frequency on captured dust at different acceleration ratio, for Silica and Potato starch.

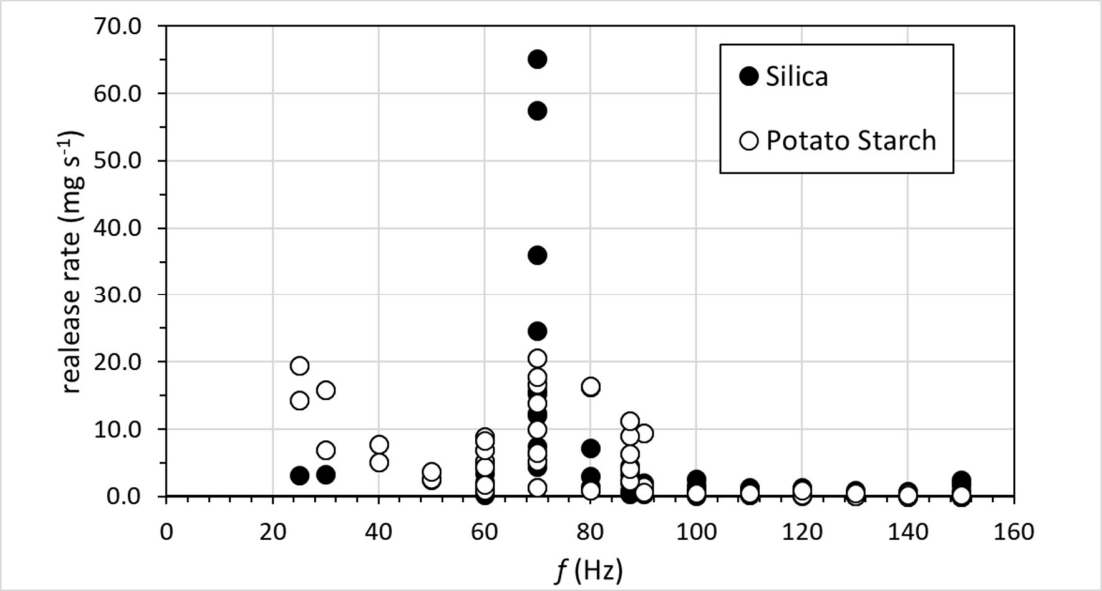


Figure 7. All the data obtained for dust release plotted as a function of the vibration frequency

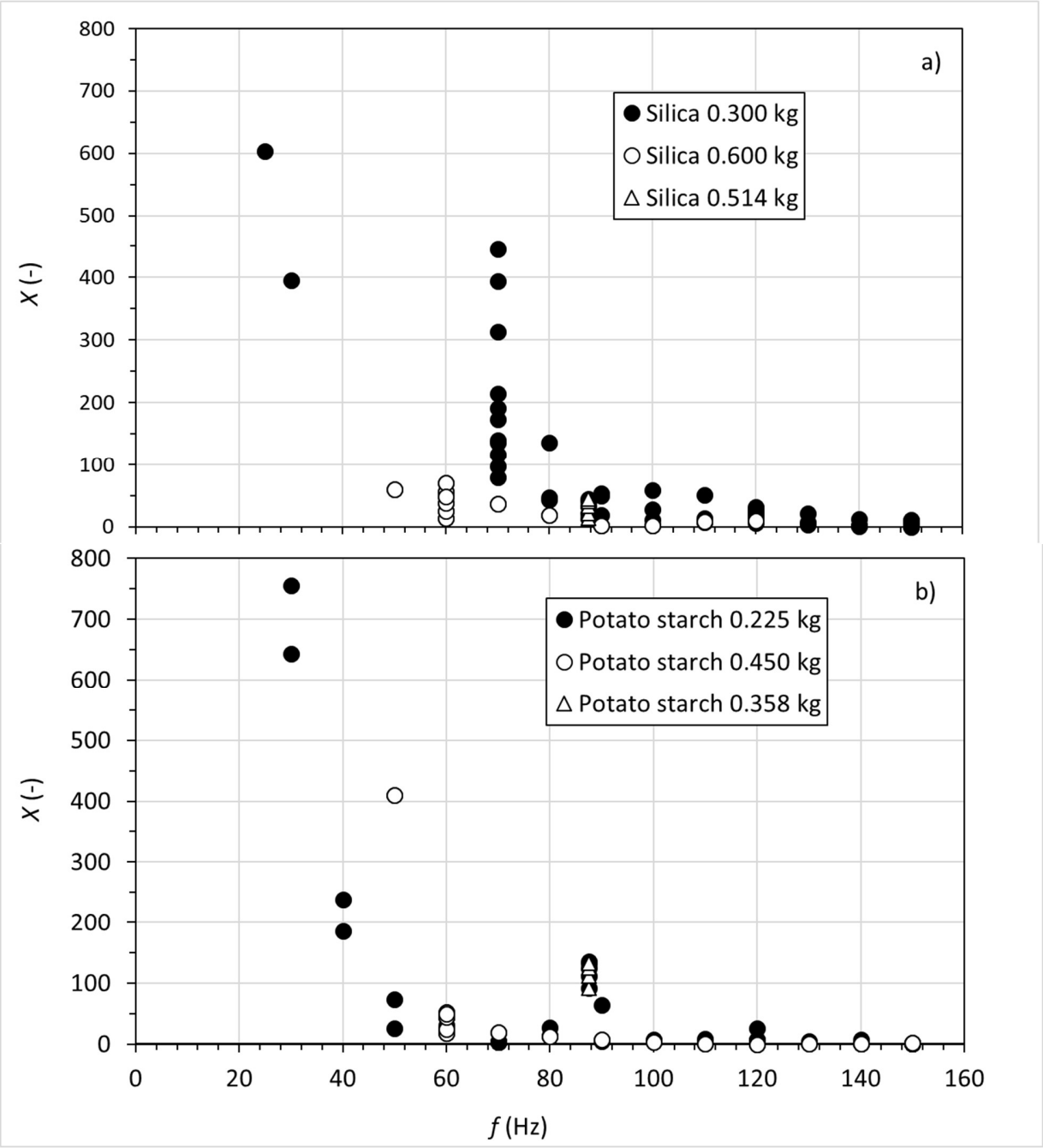


Figure 8. Dimensionless dust release rate $\chi$ reported as a function of the vibration frequency for a) Silica and b) Potato Starch.

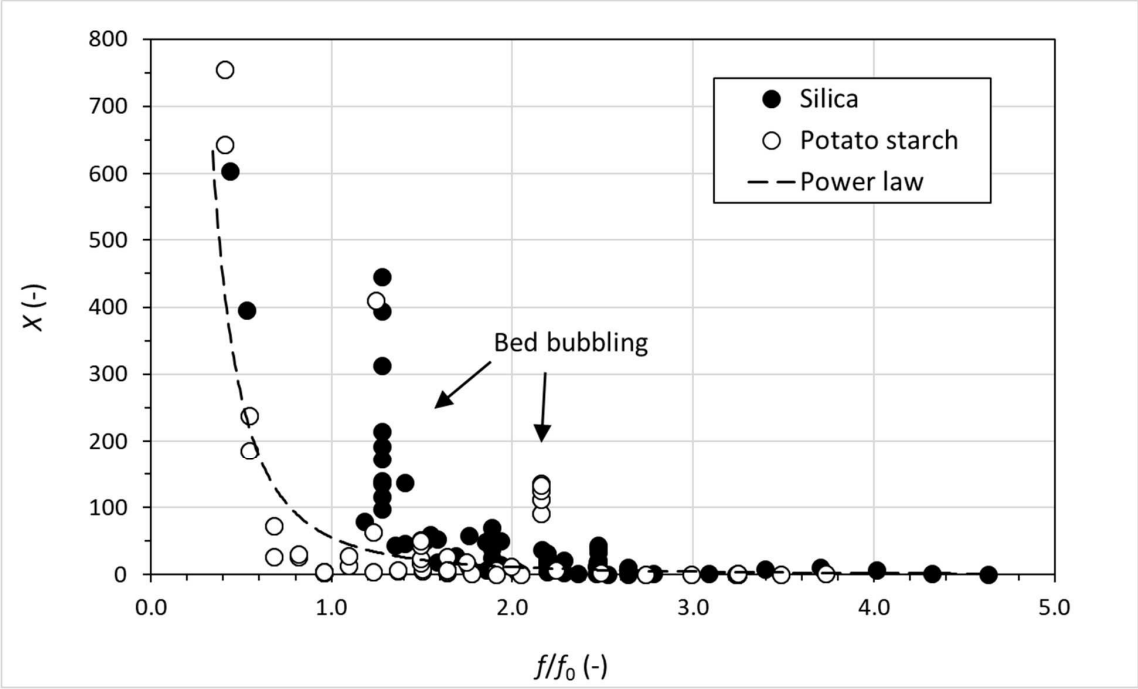


Figure 9. Dimensionless dust release rate $\chi$ reported as a function of the normalized frequency $f/f_0$ for both Silica and Potato Starch.